Dihydrogen Trioxide Clusters, $(HOOOH)_n$ ($n = 2-4$), and the Hydrogen-Bonded Complexes of HOOOH with Acetone and Dimethyl Ether: Implications for the Decomposition of HOOOH

Saša Kovačič,[†] Jože Koller,[†] Janez Cerkovnik,[†] Tell Tuttle,[‡] and Božo Plesničar*,[†]

Department of Chemistry, Faculty of Chemistry and Chemical Technology, University of Ljubljana, 1000 Ljubljana, Slovenia, and WestCHEM, Department of Pure and Applied Chemistry, University of Strathclyde, Glasgow G1 1XL, U.K.

Received: April 28, 2008; Revised Manuscript Received: June 17, 2008

Hydrogen-bonded gas-phase molecular clusters of dihydrogen trioxide (HOOOH) have been investigated using DFT (B3LYP/6-311++G(3df,3pd)) and MP2/6-311++G(3df,3pd) methods. The binding energies, vibrational frequencies, and dipole moments for the various dimer, trimer, and tetramer structures, in which HOOOH acts as a proton donor as well as an acceptor, are reported. The stronger binding interaction in the HOOOH dimer, as compared to that in the analogous cyclic structure of the HOOH dimer, indicates that dihydrogen trioxide is a stronger acid than hydrogen peroxide. A new decomposition pathway for HOOOH was explored. Decomposition occurs via an eight-membered ring transition state for the intermolecular (slightly asynchronous) transfer of two protons between the HOOOH molecules, which form a cyclic dimer, to produce water and singlet oxygen (Δ^1O_2). This autocatalytic decomposition appears to explain a relatively fast decomposition ($\Delta H_a(298K) = 19.9$ kcal/mol, B3LYP/6-311+G(d,p)) of HOOOH in nonpolar (inert) solvents, which might even compete with the water-assisted decomposition of this simplest of polyoxides ($\Delta H_a(298K) = 18.8$ kcal/mol for $(H_2O)_2$-assisted decomposition) in more polar solvents. The formation of relatively strongly hydrogen-bonded complexes between HOOOH and organic oxygen bases, HOOOH-B (B = acetone and dimethyl ether), strongly retards the decomposition in these bases as solvents, most likely by preventing such a proton transfer.

Introduction

The existence of dihydrogen trioxide (HOOOH) has in recent years been verified.[1–4] It has been demonstrated that this simplest of polyoxides, its radical $HOOO^{\bullet}$,[5] and its anion $HOOO^{-}$[6] are most likely key intermediates involved in oxidation processes that span atmospheric,[7] environmental,[8] and biological[9] systems.

Giguère et al. first reported IR and Raman spectroscopic evidence for the involvement of HOOOH in electrically dissociated mixture of water, hydrogen peroxide and oxygen.[10] More recently, Engdahl and Nelander have reported all fundamentals of HOOOH, HOOOD, and DOOOD in argon matrices by the photolysis of the HOOH(D)−ozone complex.[2] Bielski and Schwartz provided the first UV spectroscopic evidence for the existence of HOOOH in solution. They reported a UV absorption spectrum very similar to, but more intense than that of HOOH, in the pulse radiolysis of air-saturated perchloric acid solutions.[11]

Recently reported methods for the preparation of relatively highly concentrated solutions of HOOOH, i.e., ozonation of various saturated organic compounds and hydrogen peroxide in various organic solvents, allowed for the first time an unambiguous NMR (^1H and ^{17}O) spectroscopic identification and characterization of this polyoxide.[1] The ^{17}O NMR chemical shift values of HOOOH have proven particularly helpful in this respect.[1,12]

Finally, the ground-state geometry of HOOOH by using Fourier transform microwave (FTMW) spectroscopy and FTMW-mm-wave double resonance and triple resonance spectroscopy was reported. For these measurements, Endo et al. generated HOOOH in a pulsed discharge nozzle by discharging a gas mixture of oxygen and argon, passed through a reservoir filled with 30% H_2O_2 solution.[4] In the gas phase, dihydrogen trioxide is a zigzag skew-chain structure with C_2 symmetry so that both HOOO dihedral angles are equal and opposite. A number of theoretical studies on HOOOH at various levels of theory are in general agreement with these findings.[4,6c,13]

Very little of a definitive nature is known about the structure of HOOOH in solution. Our preliminary theoretical studies indicated that dimerization might be, in analogy with hydrogen peroxide, the characteristic structural feature of HOOOH in nonpolar ("inert") solvents.[14] However, for organic oxygen base solvents, the H-bonds that stabilize the dimers may be disrupted by competitive binding of HOOOH to the bases.

In the present theoretical study, we investigate the possible existence of gas-phase dihydrogen trioxide clusters, $(HOOOH)_n$ ($n = 2-4$), and, for comparison, the complexes of HOOOH with acetone and dimethyl ether, as representative oxygen bases, as well. The obtained results indicate that cyclic dimers (and perhaps trimers and tetramers) are most likely the characteristic structural feature of HOOOH in nonpolar solvents, and that this polyoxide forms relatively strong intermolecular hydrogen bonds to acetone and dimethyl ether, respectively. To explain a relatively fast decomposition of HOOOH in nonpolar solvents (toluene), as compared to the decomposition in oxygen bases,[1] we have also explored the possibility of the autocatalytic decomposition of this polyoxide to produce water and singlet oxygen (Δ^1O_2).

* Corresponding author. E-mail: bozo.plesnicar@fkkt.uni-lj.si.
[†] University of Ljubljana.
[‡] University of Strathclyde.

10.1021/jp8036928 CCC: $40.75
Published on Web 08/13/2008

Computational Methods

The equilibrium structures of dihydrogen trioxide, and its clusters, have been fully optimized at the level of density functional theory (DFT) using the B3LYP hybrid functional.[15,16] The preliminary optimizations were performed at the B3LYP/6-31G(d,p) level.[17] For an accurate estimation of the geometry and the binding energies in the complexes, the 6-311++G(3df,3pd) basis set was employed.[18] The optimization of HOOOH dimers **2A** and **2B** were also performed at the MP2/6-311++G(3df,3pd) level of theory. Vibrational frequencies (with no empirical scaling) were computed to include the zero-point-energy (ZPE), thermal, and entropic effects, as well as to ensure that all the structures correspond to true local minima (containing only positive frequencies) on the potential energy surface, and that the transition state for the decomposition of the HOOOH dimer **2A** (at B3LYP/6-311+G(d,p) level) has a single imaginary frequency (negative eigenvalue of the Hessian). The binding energy (BE) is defined as the difference of the energy of the cluster and the corresponding monomers, in their relaxed geometries. The effect of basis set superposition error (BSSE) on the calculated binding energy was estimated using the counterpoise procedure of Boys and Bernardi.[19] Because of the deficiencies of DFT when calculating O_2 ($^1\Delta_g$) we employed spin-projection[20] to provide an accurate description of the complexes involving O_2 ($^1\Delta_g$). This technique has been shown to provide reliable energetic data for complexes involving O_2 ($^1\Delta_g$)[21] and is able to reasonably reproduce (ΔE = 20.5 kcal/mol) the experimental triplet-singlet splitting of 22.5 kcal/mol.[22] The GAUSSIAN 03 program was used for the B3LYP and MP2 calculations.[23]

For benchmarking purposes, single point energy calculations have been carried out on the B3LYP/6-311++G(3df,3pd) optimized structures using RI-SCS-MP2[24] with the def2-QZVPP[25] basis set as implemented in the TurboMole program.[26] The RI-SCS-MP2 method has been shown to provide accurate energetic data with respect to binding energies and reaction energies.[24,27] In addition, the use of a large basis set in combination with the RI-SCS-MP2 method, has been demonstrated to reduce the BSSE to negligible levels; therefore we do not apply the BSSE correction to the results.[27]

Results and Discussion

The fully optimized equilibrium structures of the $(HOOOH)_n$ clusters are, together with the isolated monomers (*trans* and *cis*), shown in Figure 1 (see also Figure S1 in the Supporting Information). The optimized B3LYP/6-311++G(3df,3pd) and the corresponding MP2 structures of HOOOH agree very well with the experimentally determined structure, which exhibits C_2 symmetry with R(H−O) = 0.963 Å, R(O−O) = 1.428 Å, ∠HOO = 101.1°, ∠OOO = 107.0° and ∠HOOO = 81.8°.[4,28] The calculated binding energies are collected in Table 1. Vibrational frequencies and dipole moments of clusters **2A** and **2B** are summarized in Table 2 (for **2C-2F**, **3A**, **3B**, and **4**, see Table S1, Supporting Information).

Dimers. The HOOOH dimer **2A** is a hydrogen-bonded cyclic eight-membered ring with two hydrogen bonds and inversion symmetry (C_2). It is thus nonpolar (dipole moment, 0). The dimer **2B** is a seven-membered intermolecularly hydrogen-bonded ring structure with a dipole moment of 3.247 debye.

The variation in the binding energies predicted by B3LYP and RI-SCS-MP2 is relatively small (MAD($\Delta\Delta E$) = 0.61 kcal/mol). This is consistent with previous results indicating that B3LYP provides an accurate description of H-bonding complexes, where dispersion interactions do not play a significant role.[29] Both methods predict the same order of stability, in the case of the dimers (i.e., **2B** > **2A** > **2C** > **2D** > **2F** > **2E**). The RI-SCS-MP2 method consistently predicts greater stabilization resulting from the complex formation when the *cis*-monomers are involved (cf. trimer **3B**). This is due to the fact that in the *cis*-HOOOH monomer there is a repulsive interaction between the O−H σ^* orbitals, which is more strongly described by the RI-SCS-MP2 method. However, upon complex formation the electron density is drawn into the O···H bond, thus reducing the σ^* interaction. As a result, the complex formation is slightly more favored at the RI-SCS-MP2 level when *cis*-HOOOH is involved.

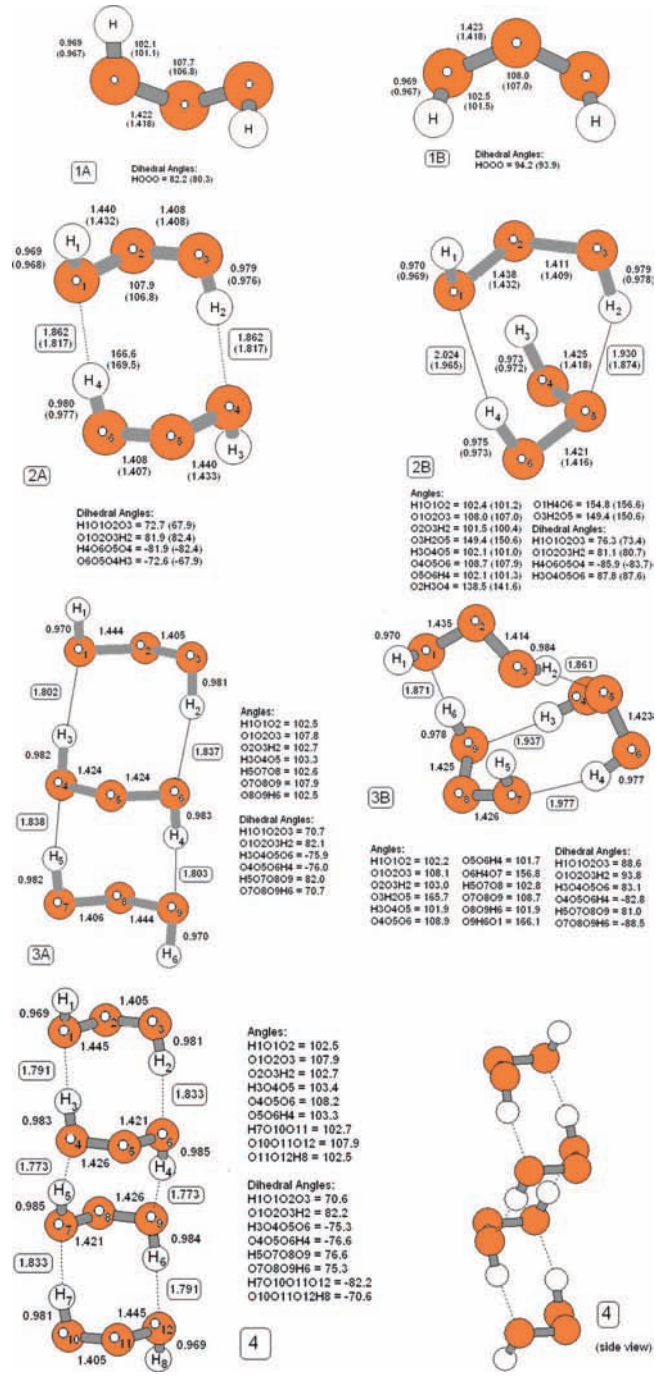

Figure 1. B3LYP optimized structures of *trans*-HOOOH (**1A**) and *cis*-HOOOH (**1B**); dimers of HOOOH, **2A** and **2B**; trimers of HOOOH, **3A** and **3B**; and the HOOOH tetramer, **4**. Bond lengths in Å and angles in degrees. Values in parentheses refer to MP2 optimized structures.

TABLE 1: Calculated Binding Energies for HOOOH and HOOH Clusters[a]

cluster (HOOOH)$_n$	ΔE	ΔH	ΔG	ΔE(SCS-MP2)[b]	$\Delta\Delta E$[c]
dimer **2A**	−8.35	−6.74	3.49	−8.50	0.15
dimer **2B**	−8.72	−6.94	3.90	−9.22	0.50
dimer **2C**	−7.02	−5.31	3.90	−7.58	0.56
dimer **2D**	−6.19	−4.57	4.27	−6.79	0.60
dimer **2E**	−5.34	−3.76	4.94	−6.12	0.78
dimer **2F**	−5.87	−4.24	4.74	−6.53	0.66
trimer **3A**	−17.70	−14.47	6.53	−18.35	0.65
trimer **3B**	−18.22	−14.52	7.83	−19.73	1.51
tetramer **4**	−26.97	−22.10	9.85	−28.42	1.45
dimer HOOH	−7.31	−5.99	3.89	−7.68	0.37

[a] Binding energies (ΔE), enthalpies (ΔH) and free enthalpies (ΔG) are reported in kcal/mol. ΔE, ΔH, and ΔG values are calculated at the B3LYP/6-311++G(3df,3pd) level of theory and include BSSE corrections. [b] ΔE(SCS-MP2) are binding energies (in kcal/mol) calculated at the RI-SCS-MP2 level of theory with the def2-QZVPP basis set. BSSE corrections are not included. [c] $\Delta\Delta E$ is the difference between the B3LYP and SCS-MP2 binding energies.

The inclusion of thermal corrections and the zero-point energy to yield ΔH results in a destabilization of the complexes. For the dimers, the destabilization is fairly consisted across the different conformation investigated and amounts to ca. 1.6−1.8 kcal/mol. Of course, the equilibria between the free and complexed HOOOH will depend on the corresponding Gibbs free enthalpies ($\Delta G = \Delta H - T\Delta S$). We have computed the entropic contributions by applying the harmonic oscillator/rigid rotor approximation. The resulting ΔG values are listed in Table 1, but they should be viewed with some caution, for two reasons. First, the computed entropic contributions refer to the gas phase and thus neglect solvation and desolvation effects in solution, which may be substantial (vida infra). Second, the harmonic oscillator/rigid rotor approximation is known to be problematic in the case of weakly bound complexes due to the large number of low-energy vibrational modes, which in turn have large contributions to the entropy. Given this situation, the computed ΔG values can not be considered quantitatively, nonetheless, the qualitative effect of the entropic contributions are clear. Complex formation will suffer from an entropic penalty because of the loss of translational and rotational degrees of freedom (ca. 10 kcal/mol at 298 K in the gas phase). In solution, these entropic effects will be less pronounced than in the gas phase due to solvation and desolvation, but they will be present to some extent. Thus, both the thermal and entropic contributions are relatively consistent across the set of dimers; we therefore concentrate in the following discussion on the variation of ΔE.

As evident from Table 1, structures **2A** and **2B** are energetically very similar at the B3LYP/6-311++G(3df,3pd) level of theory, with **2B** being energetically slightly preferred (ΔE: −8.35 kcal/mol, **2A**; −8.72 kcal/mol, **2B**). Thus, we have additionally optimized the clusters and their constituent monomers, with the MP2/6-311++G(3df,3pd) method (see Supporting Information for details). MP2 predicts somewhat greater stability for the **2B** complex ($\Delta E = -12.29$ kcal/mol; BSSE corrected) relative to **2A** ($\Delta E = -10.80$ kcal/mol; BSSE corrected). For comparison, the binding energies in the cyclic six-membered ring structure of the HOOH dimer[30] (analogous to **2A**, see Figure S2 in Supporting Information) are −7.31 kcal/mol at the B3LYP and −7.86 kcal/mol at the MP2 level. As already reported in the literature,[31] the MP2/6-311++G(3df,3pd) calculations predict greater stability for intermolecularly hydrogen-bonded complexes than the B3LYP method with the same basis set.

The difference in the binding energies, predicted by the two methods, is 2.45 and 3.57 kcal/mol, for **2A** and **2B**, respectively. This is reflected also in the shorter length of the hydrogen bonds in **2A** at the MP2 level (1.862 Å, B3LYP; 1.817 Å, MP2). The increased stability of **2B** relative to **2A** at the MP2 level can be attributed to an additional weak interaction (hydrogen bonding) between the hydrogen atom (H_3) of one HOOOH molecule and the middle oxygen atom (O_2) of the other. The distance between these two atoms is 2.242 and 2.119 Å at the B3LYP and MP2 levels, respectively.

The tighter binding in **2A** is also seen in the decreased hydrogen bond lengths, which are shorter in **2A** relative to the HOOH dimer (1.925 Å, B3LYP; 1.896 Å, MP2; see Figure S2, Supporting Information). The stronger binding interaction in the HOOOH dimer **2A**, as compared to that in the HOOH dimer,[30] indicates that the dihydrogen trioxide is a stronger proton donor (stronger acid) than hydrogen peroxide. The calculated gas-phase proton affinities of the $HOOO^-$ anion (364.4 kcal/mol) and the HOO^- anion (376.7 kcal/mol)[6c] agree with this observation. The estimated pK_a value for HOOOH is 9.5 ± 0.2 (HOOH, 11.6 in water at 20 °C).[11b]

The strength of the interaction in the dimers is reflected in the considerable perturbation that the complex formation induces in the HOOOH structure. For example, the O−H bond involved in hydrogen bonding is lengthened by 0.010 Å and the O-OH bond is shortened by 0.014 Å in **2A** (B3LYP), as compared to the isolated HOOOH (see Figure 1). At the same time, there is also a significant change in one of the dihedral HOOO angles (by 9.5°).

In addition to the geometric changes in the monomers, there are also significant shifts in the vibrational modes, in the complex, with respect to the same modes in HOOOH monomers. For example, both dimers investigated have the O−H stretches for the hydrogens involved in the hydrogen bonding, calculated at the B3LYP level, shifted to the red by 171 and 209 cm^{-1} (165 and 202 cm^{-1}, MP2) for **2A**, and 53, 97 and 181 cm^{-1} (66, 99 and 195 cm^{-1}, MP2) for **2B**. On the other hand, the HOO bending modes (B3LYP), which are strongly hindered by the formation of a cyclic structure, are all blue-shifted, for example, by 103 and 102 cm^{-1} (110 and 105 cm^{-1}, MP2) for **2A**. Similar trends in the red and blue shifts of the O−H stretching and HOO bending modes were observed in all other dimers investigated (for structures **2C**-**2F** see Figure S1 in Supporting Information). However, no significant shifts in the stretching frequencies for the O−H bonds not involved in hydrogen bonding were observed (see Table S1 in Supporting Information).

Trimers and Tetramers. We found two stable conformations for the HOOOH trimer, i.e., an open linear structure **3A** with all *trans* forms of the HOOOH monomeric units, and a cyclic structure **3B** with one *trans* and two *cis* forms of HOOOH molecules (Figure 1). The **3B** conformation is more stable than **3A** by 0.52 kcal/mol (ΔE, B3LYP). This result is again borne out in the RI-SCS-MP2 calculations, where the relative stability is increased for **3B** to 1.38 kcal/mol. As, in the case of the dimers, the discrepancy between the RI-SCS-MP2 and B3LYP results is primarily due to the difference in the relative stability of the *cis* and *trans* forms of HOOOH predicted by the two methods.

The binding energies per unit monomer in the trimers are greater than those in the dimers. That is, energetically there is a slight favorable cooperative effect in forming the longer chain structures. For example, in **2A**, the average energy per H-bond is 4.18 kcal/mol, which is increased to 4.43 kcal/mol in **3A**.

TABLE 2: Harmonic Vibrational Frequencies (cm^{-1}) with Intensities (km mol^{-1}) and Dipole Moments (Debye) of HOOOH and $(HOOOH)_2$ at the B3LYP and [MP2] Levels

$(HOOOH)_n$ ($n = 1-2$)	dipole moment (debye)	vibrational frequencies (cm^{-1}) (intensities, km mol^{-1})
HOOOH, **1A** (*trans*)	0.979	372 (124), 430 (99), 535 (26), 803 (91), 946 (3), 1391 (31), 1399 (45), 3720 (64), 3724 (3)
	[1.123]	[364 (119), 425 (113), 548 (26), 840 (72), 926 (5), 1396 (36), 1403 (53), 3782 (75), 3785 (5)]
HOOOH, **1B** (*cis*)	3.150	286 (46), 452 (108), 521 (7), 805 (110), 946 (1), 1372 (48), 1406 (30), 3719 (26), 3722 (19)
	[3.381]	[270 (54), 451 (108), 532 (5), 841 (93), 928 (1), 1379 (57), 1412 (34), 3781 (39), 3785 (16)]
dimer **2A**	0.000	57 (3), 100 (0), 116 (10), 130 (0), 205 (17), 218 (0), 360 (0), 372 (199), 523 (0), 527 (32), 734 (161), 735 (0), 786 (0), 801 (177), 957 (10), 958 (0), 1359 (86), 1363 (0), 1493 (52), 1501 (0), 3511 (0), 3549 (837), 3727 (0), 3727 (81)
	[0.000]	[55 (3), 96 (0), 121 (11), 135 (0), 222 (18), 227 (0), 356 (0), 368 (209), 536 (0), 539 (31), 753 (151), 758 (0), 826 (0), 837 (137), 938 (17), 939 (0), 1369 (106), 1373 (0), 1501 (60), 1513 (0), 3580 (0), 3617 (904), 3772 (0), 3772 (98)]
dimer **2B**	3.247	67 (1), 102 (6), 141 (1), 155 (2), 202 (19), 249 (42), 377 (91), 475 (21), 514 (1), 526 (11), 612 (103), 712 (74), 792 (54), 809 (121), 948 (0), 949 (5), 1369 (33), 1429 (74), 1480 (91), 1499 (9), 3539 (188), 3623 (187), 3666 (128), 3727 (47)
	[3.493]	[62 (1), 119 (6), 157 (1), 172 (2), 212 (17), 264 (43), 369 (94), 491 (23), 525 (1), 539 (11), 633 (104), 738 (80), 830 (48), 851 (98), 933 (10), 935 (1), 1379 (41), 1443 (86), 1479 (92), 1514 (9), 3587 (200), 3683 (184), 3715 (196), 3771 (51)]

SCHEME 1: Autocatalytic Decomposition of $(HOOOH)_2$

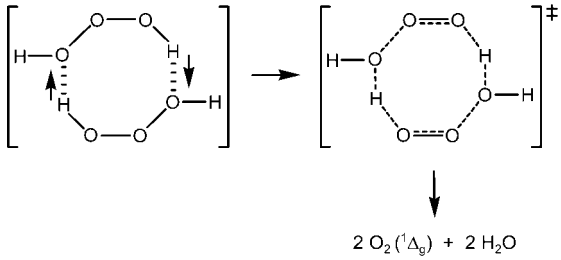

This is also reflected in shorter hydrogen bond distances, and greater red shifts of stretching frequencies of O−H bonds involved in hydrogen bonding in the trimers, as compared to the dimers (see Table S1, Supporting Information).

Only one tetramer, **4**, with a zero dipole moment, was found as a stable open linear structure on the potential energy surface (Figure 1). The intermolecular hydrogen bonds in **4** are shorter than in **3A**, indicating an even stronger interaction between the monomeric HOOOH units in this assembly. There is a further slight increase (0.06 kcal/mol) in the binding energy per H-bond relative to the **3A**.

Autocatalytic Decomposition of HOOOH. We[1,6b] and others[13e,21a] have already reported that water can catalyze decomposition of HOOOH as a bifunctional catalyst to form singlet oxygen (Δ^1O_2) and water. Although theoretical studies on the possibility of the conversion of HOOOH dimers, directly to either HOOH or the HOO•−HOOO• intermediate, and HOH have already been reported,[21a] the "simultaneous" intermolecular transfer of two hydrogen atoms in a HOOOH dimer to form $2H_2O$ and $2(\Delta^1O_2)$ has, to the best of our knowledge, not been studied by theory before (Scheme 1).

To test the hypothesis that HOOOH is capable of catalyzing its own decomposition, we have undertaken a DFT study of the intermolecular hydrogen transfer in the HOOOH dimer **2A**as a model system, at the B3LYP/6-311+G(d,p) level of theory. We found an eight-membered ring transition state (−1267 cm^{-1}), which is 19.9 kcal/mol (ΔH_a(298K)) above the energy of the HOOOH dimer. IRC calculations have been carried out on the optimized transition structure and confirm that the imaginary mode corresponds to the formation of the product complex from the reactant complex. The reaction is strongly exothermic (ΔH_r(298K) = −34.5 kcal/mol) to form the complex, $2(\Delta^1O_2) + 2H_2O$ (−26.9 kcal/mol, for isolated products).[32] The geometric parameters of the reactant complex, transition state (TS), and product complex are shown in Figure 2.

The Mulliken population analysis showed that the migrating hydrogens behave as protons. A slightly asynchronous transfer of protons was observed; i.e., one of the O−O bonds is more polarized (1.81 Å) than the other (1.78 Å) in the transition state. It is interesting to point out that comparable values of activation enthalpies for the decomposition of HOOOH, assisted by water,

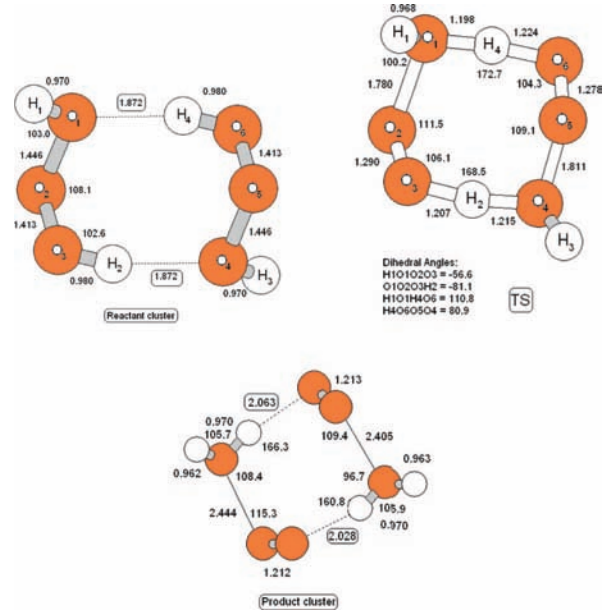

Figure 2. B3LYP/6-311+G(d,p) optimized structures of the reactant complex, the transition state (TS) for the proton transfer in $(HOOOH)_2$, and the product complex.

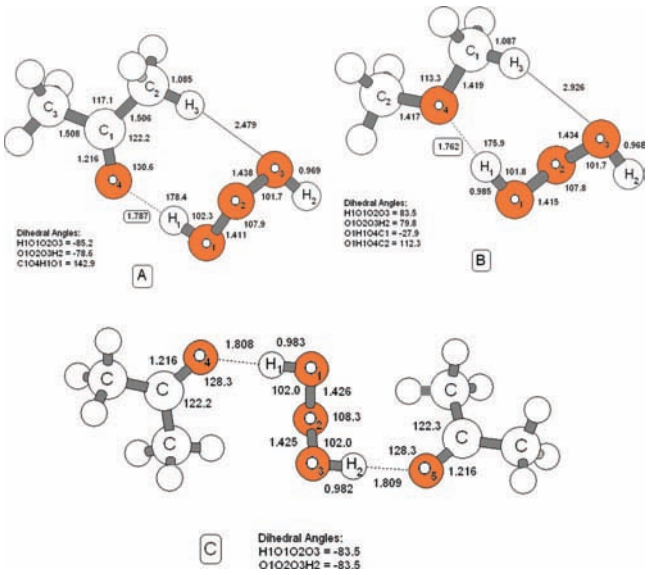

Figure 3. B3LYP optimized structures of (A) HOOOH-AC, (B) HOOOH-DME, and (C) AC-HOOOH-AC complexes. Bond lengths in Å and angles in degrees.[34]

were reported (ΔH_a(298K) = 20.0 kcal/mol, and ΔH_r(298K) = −13.1 kcal/mol for H_2O-catalyzed decomposition;[21a] ΔH_a(298K) = 17.7[21a] (18.8)[1b] kcal/mol, and ΔH_r(298K) = −13.5[21a] (−9.2)[1b] kcal/mol for $(H_2O)_2$-catalyzed decomposition (B3LYP/6-31G(d,p)). It is, therefore, quite reasonable to assume that in some higher clusters of (HOOOH)$_n$ ($n > 2$), the activation energy for the intermolecular transfer of protons might be even lower than in (HOOOH)$_2$.

Complexes of HOOOH with Acetone and Dimethyl Ether. We have already reported that HOOOH is most easily formed in the low-temperature ozonation of various saturated organic compounds in solvents with basic oxygen, i.e., esters, ethers, and ketones.[1] We have also found that this simplest of polyoxides is most stable in some of these bases (B) as solvents (particularly in ethers), most likely as a result of the formation of hydrogen-bonded complexes HOOOH-B. In addition, somewhat smaller rates for the decomposition of HOOOH in ethers, compared to the values in esters and acetone,[1] might be due to lower solubility of water in these solvents, thus enabling the formation of relatively strongly hydrogen bonded HOOOH-B complexes. Consequently, the reported water-assisted intramolecular proton transfer in HOOOH, or the intermolecular transfer of protons in the HOOOH clusters mentioned in the previous section (both resulting in the decomposition of the polyoxide to form singlet oxygen, Δ^1O_2 and water), are thus believed to be prevented, or at least strongly retarded[33] (see also Table S2 in Supporting Information).

To confirm the existence of such complexes, we report here the results of high-level theoretical studies of the interaction between HOOOH and two representative oxygen bases, i.e., acetone (AC) and dimethyl ether (DME). The optimized geometrical parameters of HOOOH-AC, HOOOH-DME, and AC-HOOOH-AC complexes are shown in Figure 3. The binding energies and harmonic frequencies of these assemblies are presented in Tables 3 and 4.

Clearly HOOOH forms relatively strongly hydrogen-bonded complexes with either of the oxygen bases investigated. The binding energy (ΔE) in the complex HOOOH-AC (−8.10 kcal/mol) is somewhat greater than that in HOOOH-DME (−7.37 kcal/mol). However, in contrast with this observation, a shorter hydrogen bond distance of 1.762 Å was calculated for the HOOOH-DME complex (1.788 Å, HOOOH-AC). Somewhat greater binding energy in HOOOH-AC, as compared to HOOOH-DME, can be explained by a weak interaction of the terminal oxygen of HOOOH with one of the hydrogen atoms of the methyl group. The intermolecular bond distance between these atoms is 2.479 Å in HOOOH-AC, but it is considerably longer in HOOOH-DME (2.926 Å).

TABLE 3: Calculated Binding Energies for the Complexes with Acetone (AC) and Dimethyl Ether (DME)[a]

HOOOH-B	ΔE	ΔH	ΔG	ΔE(SCS-MP2)[b]	$\Delta\Delta E$[c]
HOOOH-AC	−8.10	−6.53	2.46	−8.23	0.13
HOOOH-DME	−7.37	−5.68	2.30	−8.20	0.83
AC-HOOOH-AC	−15.03	−11.85	5.63	−16.30	1.27

[a] Binding energies (ΔE), enthalpies (ΔH) and free enthalpies (ΔG) are reported in kcal/mol. ΔE, ΔH, and ΔG values are calculated at the B3LYP/6-311++G(3df,3pd) level of theory and include BSSE corrections. [b] ΔE(SCS-MP2) are binding energies (in kcal/mol) calculated at the RI-SCS-MP2 level of theory with the def2-QZVPP basis set. BSSE corrections are not included. [c] $\Delta\Delta E$ is the difference between the B3LYP and SCS-MP2 binding energies.

The RI-SCS-MP2 calculations indicate that the HOOOH-AC and HOOOH-DME interactions are of similar strength, with only a slight preference for HOOOH-AC. The greater stabilization found for the HOOOH-DME complex with this method results from two factors. First, the H-bonds are generally more stable in an RI-SCS-MP2 description, relative to B3LYP. Thus, the shorter H-bond in the DME complex will have a more stabilizing effect in the RI-SCS-MP2 calculation. Second, the larger basis set will provide a better description of the weak H-bond in the DME complex. Thus, although both methods predict the HOOOH-AC complex to be the most stable, the RI-SCS-MP2 method indicates that the binding energy of the complexes will be more competitive.

In contrast to the (HOOOH)$_n$ clusters, increasing the complex size to include a second acetone unit decreases the strength of the individual H-bond. Overall, the binding energy for the AC-HOOOH-AC complex is predictably greater (ΔE = −15.03 kcal/mol) than the AC-HOOOH complex (ΔE = −8.10 kcal/mol). However, the energy per H-bond is decreased from 8.10 to 7.51 kcal/mol. This weakening of the individual H-bond is also seen in the increased H-bond length of the AC-HOOOH-AC cluster to 1.809 Å (1.787 Å in HOOOH-AC; Figure 3). The electron density is symmetric across the HOOOH unit, as indicated by the equidistant O−O bonds in the larger complex. Therefore, the interacting H atoms, are slightly less electropositive, thus decreasing the strength of the interaction with the H-bond acceptors.

A significant perturbation of dihydrogen trioxide was observed after complexation in both cases. For example, the H_1−O bond involved in hydrogen bonding is lengthened by 0.016 Å, whereas the H_1O−OOH and H_1OO−OH bonds are shortened by 0.011 Å and elongated by 0.016 Å, respectively, in the HOOOH−AC complex (Figure 3). Also, the carbon−oxygen bond in acetone part of the complex is elongated to 1.216 Å (1.209 Å in AC). The O−H stretch of the HOOOH part of the complex is red-shifted by 315 cm^{-1} in HOOOH-DME and 293 cm^{-1} in the HOOOH-AC complex, indicating a slightly stronger hydrogen bond in HOOOH-DME (Table 4).

At present, there is no direct experimental evidence for the existence of various self-associated HOOOH entities and for intermolecularly hydrogen-bonded complexes, HOOOH-B. However, a study of the temperature and concentration dependence of the OOOH ^{1}H NMR absorption of HOOOH in "inert"

TABLE 4: Harmonic Vibrational Frequencies (cm^{-1}) with Intensities (km mol^{-1}) and Dipole Moments (Debye) of HOOOH-AC and HOOOH-DME Complexes at the B3LYP Level

complexes	dipole moment (debye)	vibrational frequencies (cm^{-1}) (intensities, km mol^{-1})
HOOOH-AC	3.971	22 (1), 47 (5), 74 (2), 92 (2), 96 (0), 120 (0), 144 (2), 197 (28), 364 (92), 394 (6), 495 (1), 526(13), 553 (21), 786 (24), 795 (10), 808 (124), 890 (1), 909 (7), 954 (3), 1091 (1), 1122 (4), 1251 (67), 1371 (37), 1392 (37), 1400 (39), 1461 (3), 1462 (18), 1474 (14), 1490 (15), 1541 (32), 1765 (262), 3029 (1), 3035 (7), 3084 (3),3090 (9), 3146 (7), 3159 (0), 3427 (940), 3732 (27)
AC		35 (0), 133 (0), 381 (2), 492 (1), 537 (14), 783 (2), 886 (0), 887 (10), 1085 (0), 1120 (3), 1234 (73), 1388 (54), 1388 (19), 1460 (1), 1465 (2), 1471 (28), 1488 (19), 1790 (197), 3027 (1), 3034 (7), 3080 (0), 3088 (16), 3142 (12), 3143 (6)
HOOOH-DME	2.380	17 (1), 38 (6), 58 (1), 99 (2), 136 (3), 194 (3), 201 (13), 248 (14), 376 (92), 419 (9), 530 (15), 796 (64), 833 (74), 924 (59), 951 (3), 1109 (75), 1165 (0), 1187 (67), 1196 (6), 1275 (8), 1378 (36), 1465 (1), 1484(1),1492 (2), 1494 (17), 1496 (12), 1513 (6), 1536 (22), 2991 (44), 2999 (71), 3046 (74), 3052 (12), 3125 (15), 3137 (8), 3405 (863), 3729 (27)
DME		204 (0), 235 (5), 410 (2), 936 (37), 1116 (52), 1162 (0), 1192 (7), 1193 (95), 1267 (6), 1460 (2), 1483 (0), 1487 (0), 1491 (14), 1496 (12), 1513 (4), 2964 (60), 2975 (67), 3009 (128), 3014 (0), 3113 (30), 3114 (20)

SCHEME 2: Complexation of HOOOH with Organic Oxygen Bases (B)

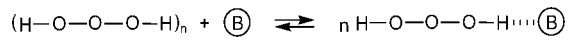

solvents (for example, toluene) and in various oxygen bases; i.e., methyl acetate, *tert*-butyl methyl ether, and acetone showed a small but definitive upfield shift of the OOOH absorption with increasing temperature, which corresponds to the appearance of larger HOOOH clusters at lower temperatures and at higher concentrations of this polyoxide[35] (see also Tables S3 and S4 in Supporting Information). A considerable downfield shift of the OOOH absorption in oxygen bases as solvents most likely reflects the formation of hydrogen-bonded complexes of HOOOH (and perhaps its clusters) with these bases (Scheme 2). The interchange between all these forms, which contributes to narrow time-averaged features, must be fast because no exchange broadening of the OOOH absorption was observed even at the lowest temperature investigated (−100 °C, in toluene-d_8 or dimethyl ether).

Conclusions

The structure, energies, and harmonic vibrational frequencies of the HOOOH clusters have been investigated by using B3LYP/6-311++G(3df,3pd), and in some cases, MP2/6-311++G(3df,3pd) level of theory. The obtained results demonstrate that HOOOH can form relatively strongly hydrogen-bonded cyclic dimers, trimers and a tetramer. In all the clusters investigated HOOOH participates as a donor as well as an acceptor for hydrogen bonds. We believe that these assemblies of HOOOH molecules represent the characteristic structural feature of this simplest of polyoxides in nonpolar ("inert") solvents (for example, toluene), as well as in the argon matrix. It is also quite possible that some of the HOOOH dimers might even survive for a short period of time in the gas phase.

The autocatalytic decomposition of HOOOH in the dimer **2A** as a model structure, to produce water and singlet oxygen (Δ^1O_2), was investigated computationally, and it was demonstrated that this type of decomposition is most likely the predominant fragmentation of HOOOH in nonpolar solvents. This decomposition pathway may even compete with water-assisted decomposition of dihydrogen trioxide in more polar solvents (for example, methyl acetate and acetone), in which water is considerably more soluble than in nonpolar solvents. The formation of relatively strongly hydrogen-bonded complexes of HOOOH with acetone and dimethyl ether, respectively, prevents the donation of the proton to the other end of the molecule (as in the HOOOH−HOH complexes) or intermolecularly between HOOOH molecules in the dihydrogen trioxide clusters, thus slowing down considerably the decomposition of the polyoxide in these organic bases as solvents.

Acknowledgment. This work was financially supported by the Slovenian Research Agency (J1-9410).

Supporting Information Available: Cartesian coordinates for all the structures investigated. The optimized gas-phase structures of the HOOH dimer and $(HOOOH)_2$ dimers, 2C-2F (Figures S1 and S2). Harmonic vibrational frequencies and dipole moments of HOOOH clusters, 2C-4 (Table S1). NMR and kinetic data for the decomposition of HOOOH in various solvents (Tables S2−S4). This material is available free of charge via the Internet at http://pubs.acs.org.

References and Notes

(1) (a) Plesničar, B.; Cerkovnik, J.; Tekavec, T.; Koller, J. *J. Am. Chem. Soc.* **1998**, *120*, 8005. (b) Plesničar, B.; Cerkovnik, J.; Tekavec, T.; Koller, J. *Chem.-Eur. J.* **2000**, *6*, 809. (c) Plesničar, B.; Tuttle, T.; Cerkovnik, J.; Cremer, D. *J. Am. Chem. Soc.* **2003**, *125*, 11553. (d) Cerkovnik, J.; Tuttle, T.; Kraka, E.; Lendero, N.; Plesničar, B.; Cremer, D. *J. Am. Chem. Soc.* **2006**, *128*, 4090.

(2) Engdahl, A.; Nelander, B. *Science* **2002**, *295*, 482.

(3) Nyffeler, P. T.; Boyle, N. A.; Eltepu, L.; Wong, C.-H.; Eschenmoser, A.; Lerner, R. A.; Wentworth, P., Jr. *Angew. Chem., Int. Ed.* **2004**, *43*, 4656.

(4) Suma, K.; Sumiyoshi, Y.; Endo, Y. *J. Am. Chem. Soc.* **2005**, *127*, 14998.

(5) (a) Cacace, F.; de Petris, G.; Pepi, E.; Troiani, A. *Science* **1999**, *285*, 81. (b) Nelander, B.; Engdahl, A.; Svensson, T. *Chem. Phys. Lett.* **2000**, *332*, 403. (c) Engdahl, A.; Nelander, B. *Science* **2002**, *295*, 482. (d) Suma, K.; Sumiyoshi, Y.; Endo, Y. *Science* **2005**, *308*, 1885. (e) Cooper, P. D.; Moore, M. H.; Hudson, R. L. *J. Phys. Chem. A* **2006**, *110*, 7985. (f) Chalmet, S.; Ruiz-Lopez, M. F. *Chem. Phys. Chem.* **2006**, *7*, 463. (g) Derro, E. L.; Murray, C.; Sechler, T. D.; Lester, M. I. *J. Phys. Chem. A* **2007**, *111*, 11592. (h) Derro, E. L.; Sechler, T. D.; Murray, C.; Lester, M. I. *J. Phys. Chem. A*, in press.

(6) (a) Nangia, P. S.; Benson, S. W. *J. Am. Chem. Soc.* **1980**, *102*, 3105. (b) Koller, J.; Plesničar, B. *J. Am. Chem. Soc.* **1996**, *118*, 2470. (c) Kraka, E.; Cremer, D.; Koller, J.; Plesničar, B. *J. Am. Chem. Soc.* **2002**, *124*, 8462. (d) Elliott, B.; Alexandrova, A. N.; Boldyrev, A. I. *J. Phys.*

Chem. A **2003**, *107*, 1203. (e) Wu, A.; Cremer, D.; Plesničar, B. *J. Am. Chem. Soc.* **2003**, *125*, 9395. (f) Cacace, F.; Cipollini, R.; de Petris, G.; Troiani, A. *Int. J. Mass Spectrom.* **2003**, *228*, 717. (g) Tuttle, T.; Cerkovnik, J.; Plesničar, B.; Cremer, D. *J. Am. Chem. Soc.* **2004**, *126*, 16093. (h) Lesko, T. M.; Colussi, A.; Hoffmann, M. R. *J. Am. Chem. Soc.* **2004**, *126*, 4432. (i) Mazziotti, D. A. *J. Phys. Chem. A* **2007**, *111*, 12635.

(7) Zheng, W.; Jewitt, D.; Kaiser, R. I. *Phys. Chem. Chem. Phys.* **2007**, *9*, 2556.

(8) (a) Xu, X.; Goddard, W. A., III. *Proc. Natl. Acad. Sci. U.S.A.* **2002**, *99*, 15308. (b) Maetzke, A.; Jensen, S. J. K. *Chem. Phys. Lett.* **2006**, *425*, 40.

(9) (a) Wentworth, P., Jr.; Jones, L. H.; Wentworth, A. D.; Zhu, X. Y.; Larsen, N. A.; Wilson, I. A.; Xu, X.; Goddard, W. A., III; Janda, K. D.; Eschenmoser, A.; Lerner, R. A. *Science* **2001**, *293*, 1806. (b) Zhu, X. Y.; Wentworth, P., Jr.; Wentworth, A. D.; Eschenmoser, A.; Lerner, R. A.; Wilson, I. A. *Proc. Natl. Acad. Sci. U.S.A.* **2004**, *101*, 2247. (c) Datta, D.; Vaidehi, N.; Xu, X.; Goddard, W. A., III. *Proc. Natl. Acad. Sci. U.S.A.* **2002**, *99*, 2636. (d) Wentworth, P., Jr.; Wentworth, A. D.; Zhu, X. Y.; Wilson, I. A.; Janda, K. D.; Eschenmoser, A.; Lerner, R. A. *Proc. Natl. Acad. Sci. U.S.A.* **2003**, *100*, 1490. (e) Shukla, P. K.; Mishra, P. C. *J. Phys. Chem. B* **2007**, *111*, 4603.

(10) (a) Arnau, J. L.; Giguère, P. A. *J. Chem. Phys.* **1974**, *60*, 270. (b) Giguère, P. A.; Srinivasan, T. K. K. *Chem. Phys. Lett.* **1975**, *33*, 479.

(11) (a) Czapski, G.; Bielski, B. H. J. *J. Phys. Chem.* **1963**, *67*, 2180. (b) Bielski, B. H. J.; Schwartz, H. A. *J. Phys. Chem.* **1968**, *72*, 3836. (c) Bielski, B. H. J. *J. Phys. Chem.* **1970**, *74*, 3213.

(12) Wu, A.; Cremer, D.; Gauss, J. *J. Phys. Chem. A* **2003**, *107*, 8737.

(13) (a) Cremer, D. *J. Chem. Phys.* **1978**, *69*, 4456. (b) Jackels, C. F.; Phillips, D. H. *J. Chem. Phys.* **1986**, *84*, 5013. Jackels, C. F. *J. Chem. Phys.* **1993**, *99*, 5768. (c) Gonzalez, C.; Theisen, J.; Zhu, L.; Schlegel, H. B.; Hase, W. L.; Kaiser, E. W. *J. Phys. Chem.* **1991**, *95*, 6784. (d) Fujii, T.; Yashiro, M.; Tokiwa, H. *J. Am. Chem. Soc.* **1997**, *119*, 12280. (e) Mckay, D. J.; Wright, J. S. *J. Am. Chem. Soc.* **1998**, *120*, 1003.

(14) Plesničar, B. *Acta Chim. Slov.* **2005**, *52*, 1.

(15) Becke, A. D. *J. Chem. Phys.* **1993**, *98*, 5648.

(16) Lee, C. T.; Yang, W.; Parr, R. G. *Phys. Rev. B* **1988**, *37*, 785.

(17) Krishnan, R.; Binkley, J. S.; Seeger, R.; Pople, J. A. *J. Chem. Phys.* **1980**, *72*, 650.

(18) Krishnan, R.; Frisch, M. J.; Pople, J. A. *J. Chem. Phys.* **1980**, *72*, 4244.

(19) Boys, S. F.; Bernardi, F. *Mol. Phys.* **1970**, *19*, 553.

(20) Wittbrodt, J. M.; Schlegel, H. B. *J. Chem. Phys.* **1996**, *105*, 6574.

(21) (a) Xu, X.; Muller, R. P.; Goddard, W. A., III. *Proc. Natl. Acad. Sci. U.S.A.* **2002**, *99*, 3376. (b) Reddy, A. R.; Bendikov, M. *Chem. Commun.* **2006**, 1179.

(22) *CRC Handbook of Chemistry and Physics on CD-ROM*, 2000 version; Lide, D. R., Ed.;CRC Press LLC; Boca Raton, FL, 2000.

(23) Frisch, M. J. et al. Gaussian 03, Rev. B.03, Gaussian, Inc.: Pittsburgh, PA, 2003.

(24) Grimme, S. *J. Chem. Phys.* **2003**, *118*, 9095.

(25) Weigend, F.; Ahlrichs, R. *Phys. Chem. Chem. Phys.* **2005**, *7*, 3297.

(26) (a) TURBOMOLE, V. 5.10, 2007. (b) Ahlrichs, R.; Bär, M.; Häser, M.; Horn, H.; Kölmel, C. *Chem. Phys. Lett.* **1989**, *162*, 165. (c) Häser, M.; Ahlrichs, R. *J. Comput. Chem.* **1989**, *10*, 104. (d) Horn, H.; Weiss, H.; Häser, M.; Ehrig, M.; Ahlrichs, R. *J. Comput. Chem.* **1991**, *12*, 1058. (e) Treutler, O.; Ahlrichs, R. *J. Chem. Phys.* **1995**, *102*, 346.

(27) Shields, A. E.; van Mourik, T. *J. Phys. Chem. A* **2007**, *111*, 13272.

(28) Mean absolute deviation (MAD) in bond lengths is 0.006 Å for B3LYP and 0.007 Å for MP2 optimized structures. The MAD in angles is 0.7° for B3LYP and 0.6° for MP2 optimized structures. CCSD(T)/6-311++G(3df,3pd) equilibrium trans-geometry of HOOOH is R(H−O) = 0.966 Å, R(O−O) = 1.423 Å, ∠HOO = 101.9°, ∠OOO = 106.8° and ∠HOOO = 81.2° (see ref 6c).

(29) Tsuzuki, S.; Lüthi, H. P. *J. Chem. Phys.* **2001**, *114*, 3949.

(30) For some more recent experimental and theoretical studies on the HOOH clusters, see: (a) Pettersson, M.; Tuominen, S.; Räsänen, M. *J. Phys. Chem. A* **1997**, *101*, 1166. (b) Engdahl, A.; Nelander, B.; Karlström, G. *J. Phys. Chem. A* **2001**, *105*, 8393. (c) Kulkarni, S. A.; Bartolotti, L. J.; Pathak, R. K. *Chem. Phys. Lett.* **2003**, *372*, 620. (d) Elango, M.; Parthasarathi, R.; Subramanian, V.; Ramachandran, C. N.; Sathyamurthy, N. *J. Phys. Chem. A* **2006**, *110*, 6294.

(31) See, for example: Miller, C. E.; Francisco, J. S. *J. Am. Chem. Soc.* **2001**, *123*, 10387.

(32) There is a minor degree of spin contamination in the TS (f_{sc} = 0.0021), whereas the product complex has a much larger contamination (f_{sc} = 0.4915). Both the relative energy of the TS and the product complex were calculated using spin-projection techniques as described in the computational methods section.

(33) Comparison of kinetic and activation parameters for the disappearance of the OOOH absorption in ^{1}H NMR spectrum: (**A**) for toluene-d_8 (10^4k, s^{-1}) 0.7 (−60 °C), 3.8 (−50 °C), 18.6 (−40 °C); E_a = 15.9 kcal mol^{-1}, log A = 12.1; (**B**) for acetone-d_6 (10^4k, s^{-1}) 0.65 (0 °C), 1.7 (10 °C), 4.8 (20 °C), 10.4 (30 °C); E_a = 15.3 kcal mol^{-1}, log A = 8.0 (see Table S2 in the Supporting Information).

(34) The optimized geometrical parameters (B3LYP/6-311++G(3df.3pd)) for the AC and DME monomers: for $(CH_3)_2C{=}O$ d(C=O) = 1.209 Å, d(C−C) = 1.514 Å, ∠CCO = 121.7°, ∠COC = 116.5°; for $(CH_3)_2O$ d(C−O) = 1.410 Å, ∠COC = 112.9°.

(35) The temperature (**A**) and concentration (**B**) dependence of the OOOH ^{1}H NMR chemical shift (in ppm relative to the tetramethylsilane): (**A**) at−70 °C 13.74 (acetone-d_6), 10.27 (toluene-d_8); at−60 °C 13.65 (acetone-d_6), 9.78 (toluene-d_8); at−50 °C 13.56 (acetone-d_6), 9.39 (toluene-d_8); at−40 °C 13.45 (acetone-d_6), 9.18 (toluene-d_8); (**B**) for acetone-d_6 55.0 mM, 12.92; 29.0 mM, 12.88; 9.2 mM, 12.83; 0.65 mM, 12.83. (See also Tables S3 and S4 in the Supporting Information.)

JP8036928